64 (2019) APPLICATIONS OF MATHEMATICS No. 5, 501–530

DG METHOD FOR PRICING EUROPEAN OPTIONS UNDER MERTON JUMP-DIFFUSION MODEL

Jiří Hozman, Liberec, Tomáš Tichý, Ostrava,
Miloslav Vlasák, Praha

Received November 2, 2018. Published online October 1, 2019.

Abstract. Under real market conditions, there exist many cases when it is inevitable to adopt numerical approximations of option prices due to non-existence of analytical formulae. Obviously, any numerical technique should be tested for the cases when the analytical solution is well known. The paper is devoted to the discontinuous Galerkin method applied to European option pricing under the Merton jump-diffusion model, when the evolution of the asset prices is driven by a Lévy process with finite activity. The valuation of options under such a model with lognormally distributed jumps requires solving a parabolic partial integro-differential equation which involves both the integrals and the derivatives of the unknown pricing function. The integral term related to jumps leads to new theoretical and numerical issues regarding the solving of the pricing equation in comparison with the standard approach for the Black-Scholes equation. Here we adopt the idea of the relatively modern technique that the integral terms in Merton-type models can be viewed as solutions of proper differential equations, which can be accurately solved in a simple way. For practical purposes of numerical pricing of options in such models we propose a two-stage implicit-explicit scheme arising from the discontinuous piecewise polynomial approximation, i.e., the discontinuous Galerkin method. This solution procedure is accompanied with theoretical results and discussed within the numerical results on reference benchmarks.

Keywords: option pricing; Merton jump-diffusion model; integro-differential equation; discontinuous Galerkin method; semi-implicit discretization; a priori error estimates

MSC 2010: 65M60, 35Q91, 65M15, 91G60, 91G80

The first two authors were supported through the Czech Science Foundation (GA ČR) under project 16-09541S. Furthermore, the second author also acknowledges the support provided within SP2019/5, an SGS research project of VŠB-TU Ostrava. The research of the third author was supported by grant 17-01747S of the Czech Science Foundation; he is a junior member of the university center for mathematical modeling, applied analysis and computational mathematics (MathMAC). The support is greatly acknowledged.

DOI: 10.21136/AM.2019.0305-18

1. Introduction

One of the most important applications of advanced mathematics in finance is related to pricing of financial derivatives and especially options due to their complex payoff functions (see also [20] or [21]). In general, the modern pricing methods, that date back to [5] and [29], are based on no-arbitrage arguments and can help various participants of the market to recover correct prices and keep a balance between the supply and demand. On the contrary, without efficient pricing procedures the stability of the prices would be threatened.

In the simplest cases of the Gaussian distribution, the pricing method can lead to analytical solutions. However, the empirical observations show that the returns of financial asset prices are not normally distributed—instead, the fat tails and asymmetry are present. In order to cope with these facts, one can consider either stochastic volatility, probability distribution with more parameters, or jumps (or their combination), see e.g. [8] for a review. In these cases, however, the analytical solution can be hardly attainable and some of the numerical approaches must be adopted. The commonly used techniques are, for example, Monte Carlo simulation (see e.g. [6]), lattices and trees (for the first time formulated in [10]), finite difference [37] or finite element methods [1].

In this contribution we focus on the jump-diffusion model, for the first time introduced by Merton in [30] and extended, among others, by Kou in [24]. For a complex overview, see [8]. Specifically, we consider European-style options on a single asset, price of which is driven by a Lévy model with finite activity, and numerically evaluate the options by solving the relevant partial integro-differential equation (PIDE). This complex governing equation with a combination of differential and integral terms has been already treated by various numerical methods based on finite difference [9], finite volume [38] and finite element techniques [2]. Unlike these methods, we propose a two-stage implicit-explicit time stepping scheme combined with the discontinuous Galerkin spatial discretization. Moreover, the accurate and simple evaluation of the integral term is performed as solving a proper PDE, see the inspiring idea in [7].

The discontinuous Galerkin (DG) method was developed in the early 1970s (see the technical report [32]) and it was successfully profiled in the field of computational fluid dynamics, cf. [12]. Its potency in option pricing problems has not yet been fully exploited, especially as concerns advanced option pricing models. Apart from our recent research [18], [19], [20], [21], and [22], let us quote from very little material published in the literature, at least papers [27] and [31].

Our approach improves the numerical valuation process for Merton-type jump-diffusion models in several regards:

(i) since the nonlocal integral term, which is non-stiff, is treated explicitly, the resulting linear algebra systems are sparse and therefore easier to solve;

(ii) discontinuous approximations resolve option values and sensitivity measures more properly, e.g. a piecewise (linear) payoff function has a discontinuous derivative or discrete observations can be easily implemented;

(iii) since the differential part of PIDE is represented by the convection-diffusion equation that may be convection dominated depending on the parameters of the problem, the piece-wise discontinuous character of the DG solution enables to apply the upwind stabilization that is natural in the finite volume methods;

(iv) the evaluation of the integral term as the solution of the auxiliary PDE leads to the uniform approach to the complete problem through the numerical solution of PDEs, which exhibits several advantages, either practical or theoretical, e.g., uniform implementation of discretization of the complete problem, uniform a priori or a posteriori analysis.

It can be expected that other advantages of the DG approach will be much more apparent when considering the generalizations of the model, e.g., more uncorellated underlying assets, non-constant, wide ranging model parameters and particularly complex payoff functions and market conditions (discrete barriers, American-style constraints, penalty techniques, etc.). The promising steps within Black-Scholes settings and stochastic volatility models are presented in [22].

To provide a credible numerical verification of properties of the scheme derived, this method is presented on the fundamental jump-diffusion model, for which there are a number of benchmarks and also an exact solution is known in the semi-closed form of an infinite series. In line with the above, the presented numerical experiments illustrate the significant capabilities of the proposed numerical approach, especially its robustness with respect to the model parameters.

The paper is organized as follows. In Section 2 we introduce the relevant governing equation and define its variational formulation on a bounded domain. Next, in Section 3 the numerical scheme is developed, followed by its error analysis in Section 4. Finally, in Section 5, the convergence properties and robustness of the proposed numerical scheme are demonstrated on reference numerical experiments.

2. Merton jump-diffusion model

We consider here European-style options on an underlying asset S, i.e., options exercising of which is permitted only at maturity time T. Such options exist either as put (right to sell) or call (right to buy) options and their value at maturity can

be represented as a payoff function

$$\max(S-\mathcal{K},0) \quad \text{(call)}, \qquad \max(\mathcal{K}-S,0) \quad \text{(put)}, \tag{2.1}$$

where $\mathcal{K}$ denotes the specified price at which an option contract can be exercised, usually called the strike price. These options are called plain vanilla options due to the simplicity of the payoff function. Despite this simplicity, the payoff function is not linear and makes the pricing procedure quite challenging (compare with the linear payoff of other financial derivatives, such as forwards of swaps).

Let us denote by $V(S,t)$ the price of an option contract at time t written on the underlying asset S, whose movement is represented by a combination of the Brownian motion with drift and a compound Poisson process $\mathrm{d}J$ (for survey see [8]), i.e., by a Lévy process of the form

$$\mathrm{d}S = (r-\lambda\kappa)S\,\mathrm{d}t + \sigma S\,\mathrm{d}W + \zeta S\,\mathrm{d}J, \tag{2.2}$$

where r is the instantaneous expected return on asset S (represented by a risk-free interest rate), σ is the instantaneous volatility of the return, λ is the Poisson arrival intensity, ζ is an impulse function giving a jump from S to $(\zeta+1)S$ and κ is the expectation $E(\zeta)$ of the random variable ζ. The Wiener process $\mathrm{d}W$ is assumed to be independent of the Poisson process $\mathrm{d}J$. If $\lambda = 0$, then the asset dynamics (2.2) is identical to the Black-Scholes (BS) model [5]. In contrast, (2.2) reduces to a pure jump process for $\sigma = 0$. In the rest of the paper, we assume $\sigma > 0$ and $\lambda > 0$.

The model originally presented by Merton [30] is a special case of the jump-diffusion model (2.2), where jumps are lognormally distributed, i.e., $\ln(\zeta+1) \sim N(\mu,\gamma^2)$ with the probability density function

$$g(y) = \frac{1}{\sqrt{2\pi}\gamma}\exp\Big(-\frac{(y-\mu)^2}{2\gamma^2}\Big) \quad \text{for } \zeta = \mathrm{e}^y. \tag{2.3}$$

The fundamental result for advanced option pricing techniques under the Merton jump-diffusion model characterizes $V(S,t)$ as a solution of a deterministic partial integro-differential equation, see Subsection 2.1.

2.1. Governing equations. Similarly to the BS framework, the contingent claim V is priced using an arbitrage-free principle, Itô calculus, elimination of stochastic fluctuations and a construction of a sophisticated portfolio. Following [8], the option price V at time $t \in (0,T)$ under the Merton model (2.2)–(2.3) can be

represented in general as a solution of the backward PIDE

$$\frac{\partial V}{\partial t}(S,t)+\frac{1}{2}\sigma^2S^2\frac{\partial^2V}{\partial S^2}(S,t)+rS\frac{\partial V}{\partial S}(S,t)-rV(S,t) + \int_{\mathbb{R}}\Big[V(S\mathrm{e}^y,t)-V(S,t)-S(\mathrm{e}^y-1)\frac{\partial V}{\partial S}(S,t)\Big]\nu(\mathrm{d}y)=0 \tag{2.4}$$

in $(0,\infty)\times(0,T)$ with Lévy measure $\nu(\,\mathrm{d}y)=\lambda g(y)\,\mathrm{d}y$ and the terminal condition as the payoff function (2.1). Using the definition of the Lévy measure with (2.3) one obtains $\int_{\mathbb{R}}=\nu(\,\mathrm{d}y)=\lambda$, which exactly means that the Lévy process (2.2) is of a finite activity, in other words, it generates a finite number of jumps within any finite time interval.

For further analysis it is suitable to change asset values S to the scaled logarithmic ones x and time t to the time to maturity $\hat{t}$, i.e.,

$$x=\ln(S/\mathcal{K}),\quad \hat{t}=T-t,\quad \widehat{u}(x,\hat{t})=V(\mathcal{K}\mathrm{e}^x,T-\hat{t})/\mathcal{K}. \tag{2.5}$$

By change of variables (2.5) we obtain a new pricing function $\widehat{u}(x,\hat{t})$ satisfying

$$\frac{\partial\widehat{u}}{\partial\hat{t}}+\mathcal{D}(\widehat{u})=\mathcal{I}(\widehat{u})\quad\text{in }\mathbb{R}\times(0,T) \tag{2.6}$$

with a locally acting differential operator and a generally nonlocal integral operator

$$\mathcal{D}(\widehat{u})=-\frac{\sigma^2}{2}\frac{\partial^2\widehat{u}}{\partial x^2}-\Big(r-\frac{\sigma^2}{2}-\lambda\kappa\Big)\frac{\partial\widehat{u}}{\partial x}+(r+\lambda)\widehat{u}, \tag{2.7}$$

$$\mathcal{I}(\widehat{u})=\lambda\int_{\mathbb{R}}\widehat{u}(x+y,\hat{t})g(y)\,\mathrm{d}y, \tag{2.8}$$

where $\kappa=\int_{\mathbb{R}}(\mathrm{e}^y-1)g(y)\,\mathrm{d}y=\exp(\mu+\frac{1}{2}\gamma^2)-1$. Simultaneously to (2.6)–(2.8), it is necessary to prescribe the initial condition given by the corresponding payoff function (2.1), transformed according to (2.5) as

$$\widehat{u}_0(x)=\begin{cases}\max(\mathrm{e}^x-1,0) & \text{for a call,}\\ \max(1-\mathrm{e}^x,0) & \text{for a put.}\end{cases} \tag{2.9}$$

Since the Cauchy problem (2.6)–(2.8) with (2.9) is defined on the unbounded spatial domain $\mathbb{R}$, the asymptotic values of u are consistent with the theoretical European option prices as $S\to0+$ and $S\to\infty$, see [16], i.e.,

$$\lim_{x\to-\infty}\widehat{u}(x,\hat{t})=0,\quad \lim_{x\to\infty}\{\widehat{u}(x,\hat{t})-(\mathrm{e}^x-\mathrm{e}^{-r\hat{t}})\}=0,\quad \hat{t}>0\quad\text{(call)}, \tag{2.10}$$

$$\lim_{x\to-\infty}\{\widehat{u}(x,\hat{t})-(\mathrm{e}^{-r\hat{t}}-\mathrm{e}^x)\}=0,\quad \lim_{x\to\infty}\widehat{u}(x,\hat{t})=0,\quad \hat{t}>0\quad\text{(put)}. \tag{2.11}$$

2.2. Variational formulation on a bounded interval. The proposed pricing methodology is related to numerical solving the PIDE, which requires truncation of the domain $\mathbb{R}$ to a bounded interval $\Omega = (x_{\min}, x_{\max})$, where $x_{\min} < 0$ and $x_{\max} > 0$ stand for the minimal and maximal scaled logarithmic asset price, respectively. Without loss of generality, we will assume that $x_{\min} = -x_{\max}$ in the rest of the paper.

To localize the original problem (2.6)–(2.9) to the bounded open interval $(-x_{\max}, x_{\max})$ we follow the approach from [9]. In the first instance we define $u_R(x, \hat{t})$ as the solution of the following problem reflecting (2.10) and (2.11), i.e.,

$$\frac{\partial u_R}{\partial \hat{t}} + \mathcal{D}(u_R) = \mathcal{I}(u_R) \quad \text{in } \Omega \times (0, T) \tag{2.12}$$

with the initial and an artificial (knock-out) conditions

$$u_R(x, 0) = \widehat{u}_0(x) \quad \text{in } \Omega, \tag{2.13}$$

$$u_R(x, \hat{t}) = \mathrm{e}^{-r\hat{t}} \widehat{u}_0(x + r\hat{t}) \quad \text{in } \mathbb{R} \setminus \Omega. \tag{2.14}$$

As pointed out in [15], we approximate the original option contract (2.6)–(2.9) by the artificial one (2.12)–(2.14), which pays a rebate corresponding to the discounted and shifted payoff (2.14), cf. [2].

In what follows, we discuss estimates from [9] for the localization error based on the probabilistic approach from [4]. Supposing European put options under Merton jump-diffusion model, the following assumptions are fulfilled:

(A1) The function $\widehat{u}_0(x)$ is bounded in $\mathbb{R}$.

(A2) There exists $\alpha > 0$ such that $\int_{|y|>1} \mathrm{e}^{\alpha|y|} g(y)\,\mathrm{d}y < \infty$.

Then we can apply the general result from [9] and state the relationship between the solution $\widehat{u}$ of (2.6)–(2.9) and the solution u_R of (2.12)–(2.14) as

$$|\widehat{u}(x, \hat{t}) - u_R(x, \hat{t})| \leqslant C \operatorname{ess\,sup} \widehat{u}_0 \exp(-\alpha\delta x_{\max}) \quad \text{for } |x| \leqslant (1 - \delta) x_{\max}, \tag{2.15}$$

where the constant C does not depend on $x_{\max}$ and $\delta \in (0, 1)$ independent of $x_{\max}$. This estimate illustrates that the localization error decreases with the size of $|\Omega|$. As noted above this result holds directly for the case of put options, where $\operatorname{ess\,sup} \widehat{u}_0 = 1$. For the case of call options, $\widehat{u}_0(x)$ is unbounded in $\mathbb{R}$ and the approach is quite different. Since the call option does not allow direct application of the result (2.15) due to (A1), similar estimates for calls are obtained by a transformation of the pricing problem using the put-call parity

$$V_{\text{call}}(S, t) - V_{\text{put}}(S, t) = S - \mathcal{K}\mathrm{e}^{-r(T-t)}. \tag{2.16}$$

In the next paragraph we describe the non-local character of the integral term $\mathcal{I}u_R$ in (2.12) in more detail. First we split the integral term in two parts, make change of variables $z = x + y$ and use the condition (2.14), then we can write

$$\begin{aligned}(2.17)\quad \mathcal{I}(u_R)(x,\hat{t}) &= \lambda\int_\Omega u_R(z,\hat{t})g(z-x)\,\mathrm{d}z + \lambda\int_{\mathbb{R}\setminus\Omega} u_R(z,\hat{t})g(z-x)\,\mathrm{d}z\\ &= \lambda\int_{\mathbb{R}} u_R^e(z,\hat{t})g(z-x)\,\mathrm{d}z + \lambda\mathrm{e}^{-r\hat{t}}\int_{\mathbb{R}\setminus\Omega}\widehat{u}_0(z+r\hat{t})g(z-x)\,\mathrm{d}z\\ &= \mathcal{I}_R(u_R)(x,\hat{t}) + \mathcal{R}(x,\hat{t}),\end{aligned}$$

where

$$(2.18)\qquad u_R^e(z,\hat{t}) = \begin{cases} u_R(z,\hat{t}), & z\in\Omega,\\ 0, & z\in\mathbb{R}\setminus\Omega.\end{cases}$$

The operator $\mathcal{I}_R$ represents the restricted version of the integral operator $\mathcal{I}$ and the function $\mathcal{R}(x,\hat{t})$ its remaining part. Suppose $x_{\max} \geqslant rT$ and consider the case of a call option. Using the properties of the moment generating function of a normal random variable and after some manipulations, the function $\mathcal{R}(x,\hat{t})$ can be expressed as

$$\begin{aligned}(2.19)\quad \mathcal{R}(x,\hat{t}) &= \lambda\int_{x_{\max}}^{\infty}(\mathrm{e}^z - \mathrm{e}^{-r\hat{t}})g(z-x)\,\mathrm{d}z\\ &= \frac{\lambda\mathrm{e}^x}{\sqrt{2\pi}\gamma}\int_{x_{\max}-x}^{\infty}\mathrm{e}^y\exp\Big(-\frac{(y-\mu)^2}{2\gamma^2}\Big)\,\mathrm{d}y\\ &\quad -\frac{\lambda\mathrm{e}^{-r\hat{t}}}{\sqrt{2\pi}\gamma}\int_{x_{\max}-x}^{\infty}\exp\Big(-\frac{(y-\mu)^2}{2\gamma^2}\Big)\,\mathrm{d}y\\ &= \frac{\lambda\mathrm{e}^x\mathrm{e}^{\mu+\gamma^2/2}}{\sqrt{2\pi}\gamma}\int_{x_{\max}-x}^{\infty}\exp\Big(-\frac{(y-(\mu+\gamma^2))^2}{2\gamma^2}\Big)\,\mathrm{d}y\\ &\quad -\lambda\mathrm{e}^{-r\hat{t}}\Phi\Big(-\frac{x_{\max}-x-\mu}{\gamma}\Big)\\ &= \lambda\Big[(\kappa+1)\mathrm{e}^x\Phi\Big(\frac{x-x_{\max}+\mu+\gamma^2}{\gamma}\Big) - \mathrm{e}^{-r\hat{t}}\Phi\Big(\frac{x-x_{\max}+\mu}{\gamma}\Big)\Big],\end{aligned}$$

where Φ denotes the cumulative distribution function of the standard normal distribution. A similar approach for put options leads to the expression

$$\begin{aligned}(2.20)\quad \mathcal{R}(x,\hat{t}) &= \lambda\int_{-\infty}^{-x_{\max}}(\mathrm{e}^{-r\hat{t}} - \mathrm{e}^z)g(z-x)\,\mathrm{d}z\\ &= \lambda\Big[\mathrm{e}^{-r\hat{t}}\Phi\Big(-\frac{x+x_{\max}+\mu}{\gamma}\Big) - (\kappa+1)\mathrm{e}^x\Phi\Big(-\frac{x+x_{\max}+\mu+\gamma^2}{\gamma}\Big)\Big].\end{aligned}$$

Consequently, taking all the above into account, it is possible to represent the option pricing problem (OPP) as the initial-boundary value problem (restricted to Ω) for the unknown function $u(x,\hat{t})\colon\ \Omega\times(0,T)\to\mathbb{R}_0^+$ governed by

$$\frac{\partial u}{\partial \hat{t}}+\mathcal{D}(u)=\mathcal{I}_R(u)+\mathcal{R}\quad\text{in }\Omega\times(0,T) \tag{2.21}$$

with the initial condition

$$u(x,0)=\widehat{u}_0(x)\quad\text{in }\Omega \tag{2.22}$$

and boundary conditions

$$u(x_{\min},\hat{t})=u_L(\hat{t})=\begin{cases}0 & \text{for a call,}\\ \mathrm{e}^{-r\hat{t}}-\mathrm{e}^{-x_{\max}} & \text{for a put,}\end{cases} \tag{2.23}$$

$$u(x_{\max},\hat{t})=u_U(\hat{t})=\begin{cases}\mathrm{e}^{x_{\max}}-\mathrm{e}^{-r\hat{t}} & \text{for a call,}\\ 0 & \text{for a put.}\end{cases} \tag{2.24}$$

The integral operator $\mathcal{I}_R$ is defined in (2.17) and the function $\mathcal{R}(x,\hat{t})$ plays a role as an artificial source term, given by (2.19) or (2.20) according to the type of the option.

The boundary conditions (2.23)–(2.24) are set artificially in accordance with the asymptotic behaviour of options (2.10)–(2.11) and the localized problem (2.12)–(2.14). We prescribed here the Dirichlet type of boundary conditions at both endpoints, which are inaccurate in general. However, this fact has no effect on the results of the pricing process if we guarantee that the zone of financial interest, i.e., the domain $\Omega^*\subset\Omega$ in which option values are desirable to know, is sufficiently distant from the far-field boundary $\partial\Omega$. More precisely, the solution of (OPP) represents a solution of the localized problem (2.12)–(2.14) restricted to Ω, which is related to the original problem through error estimates (2.15) reflecting the fact that the localization error is the most apparent near the boundary $\partial\Omega$.

Next, we derive the variational formulation to (OPP) and establish its well-posedness. First, we recall the well-known Lebesgue space $L^2(\Omega)$ with the induced norm $\|\cdot\|=(\cdot,\cdot)^{1/2}$ by the inner product $(\cdot,\cdot)$, and Sobolev spaces $H^1(\Omega)$ and $H_0^1(\Omega)=\{v\in H^1(\Omega)\colon\ v(x_{\min})=v(x_{\max})=0\}$. For the detailed definition of Lebesgue, Sobolev and Bochner spaces we refer to the book [25]. Also note that the results (2.15) can be extended in the sense of L^2-norm and H^1-norm, see [28].

In order to cast (OPP) in a weak sense we consider a test function $v\in\mathcal{C}_0^\infty(\Omega)$ and multiply (2.21) by v. Since the space $\mathcal{C}_0^\infty(\Omega)$ is densely embedded in $H_0^1(\Omega)$, using

integration by parts, we obtain

$$\frac{\mathrm{d}}{\mathrm{d}\hat{t}}(u,v)+(\mathcal{D}_R(u),v)=(\mathcal{I}_R(u),v)+(\mathcal{R},v)\quad\forall\, v\in H_0^1(\Omega),\ \text{a.e. } \hat{t}\in(0,T) \tag{2.25}$$

with forms

$$(\mathcal{D}_R(u),v)=\frac{\sigma^2}{2}\int_\Omega\frac{\partial u}{\partial x}\frac{\partial v}{\partial x}\,\mathrm{d}x+\Big(\lambda\kappa+\frac{\sigma^2}{2}-r\Big)\int_\Omega\frac{\partial u}{\partial x}v\,\mathrm{d}x + (r+\lambda)\int_\Omega uv\,\mathrm{d}x, \tag{2.26}$$

$$(\mathcal{I}_R(u),v)=\lambda\int_\Omega\Big(\int_{\mathbb{R}}u^e(x+y,\hat{t})g(y)\,\mathrm{d}y\Big)v\,\mathrm{d}x, \tag{2.27}$$

$$(\mathcal{R},v)=\int_\Omega\mathcal{R}(x,\hat{t})v\,\mathrm{d}x, \tag{2.28}$$

where $u^e(\hat{t})$ denotes the zero extension of the function $u(\hat{t})$ with support in Ω to all of $\mathbb{R}$, cf. (2.18).

Note that the logarithmic spatial coordinates and the bounded domain Ω guarantee the well-posedness of (2.26) and (2.27) in the space $H^1(\Omega)$ and overcome the undesirable degeneracy of (2.4) at the left endpoint $S=0$, cf. the different treatment via the weighted Sobolev spaces [1]. Now, we are ready to introduce the concept of a weak solution.

Definition 2.1. The variational formulation of (OPP) reads:

Find $u\in L^2(0,T;H^1(\Omega))\cap H^1(0,T;H^{-1}(\Omega))$ such that the following conditions are satisfied:

$$u-u_D\in L^2(0,T;H_0^1(\Omega)),\ \text{where } u_D(\hat{t})\in H^1(\Omega)\ \text{such that} \tag{2.29}$$
$$u_D(\hat{t})\big|_{x=x_{\min}}=u_L(\hat{t})\ \text{and}\ u_D(\hat{t})\big|_{x=x_{\max}}=u_U(\hat{t})\ \text{a.e. } \hat{t}\in(0,T),$$

$$\Big(\frac{\partial u}{\partial\hat{t}}(\hat{t}),v\Big)+(\mathcal{D}_R(u(\hat{t})),v)=(\mathcal{I}_R(u(\hat{t})),v)+(\mathcal{R}(\hat{t}),v) \tag{2.30}$$
$$\forall\, v\in H_0^1(\Omega),\ \text{a.e. } \hat{t}\in(0,T),$$

$$(u(0),v)=(\widehat{u}_0,v)\quad\forall\, v\in H_0^1(\Omega). \tag{2.31}$$

Interested reader can consult, e.g., [15] and [28] for alternative definitions of the variational formulation of PIDE associated with jump-diffusion models.

Theorem 2.1. *Problem* (2.29)–(2.31) *has a unique weak solution.*

P r o o f. The proof follows the same lines as in [28] and results from Theorem 2.3 and Theorem 3.4, introduced in that paper. □

3. Discretization

Unlike the BS framework, pricing of options under jump-diffusion processes requires solving various PIDEs. This is challenging since the integral part arising from jumps leads to new theoretical and numerical issues. Moreover, the differential part exhibits a convection-diffusion character that can be convection dominated depending on the choice of parameters of the problem. In such a situation, the problem has to be carefully handled numerically and classical methods like the finite element method and the finite difference method may have serious difficulties to solve these problems correctly, since spurious oscillations may appear in the solution, see, e.g., [34].

From this point of view, the DG method applied to (OPP) represents a very promising numerical tool in these issues, compared to commonly used techniques. This approach provides the numerical solution of the PIDE composed of piecewise polynomial functions on the finite element mesh without any requirements on the continuity of the solution between the particular elements, for a detailed overview see [12] and [33]. Discontinuous approximations enable to apply natural upwind stabilization in interelement communications well known from the finite volume method, which allows the resulting method to solve (OPP) uniformly for a high range of parameters without any restrictions on the mesh size. On the other hand, the higher polynomial degree approximations allow efficient solution of the underlying problem due to higher convergence rates. DG approximations possess other benefits in comparison with the finite element method or the finite difference method which are even more apparent for more difficult problems that may arise from the generalization of (OPP), e.g., the method is simpler to parallelize or adaptive procedures are easier to apply.

This section is organized as follows. We first introduce a partition of Ω and the appropriate function spaces defined over this partition. The application of a method of lines as a space semidiscretization technique on (OPP) is then discussed, coupled with a two-stage implicit-explicit time stepping scheme. The important part is the evaluation of the integral term. Finally, we summarize all the above into a solution procedure consisting of several linear systems solved by the appropriate iterative method.

3.1. Partitions and function spaces. Let $\mathcal{T}_h$ $(h > 0)$ be a family of partitions of the closure $\overline{\Omega} = [x_{\min}, x_{\max}]$ of the domain Ω into N closed subintervals $I_k = [x_{k-1}, x_k]$ with lengths $h_k := x_k - x_{k-1}$. Then we set $\mathcal{T}_h = \{I_k, 1 \leqslant k \leqslant N\}$ with the spatial step $h = \max\limits_{1 \leqslant k \leqslant N} h_k$ and call the interval I_k an element. We additionally

assume that the condition of a local quasi-uniformity is satisfied, which here means that the lengths of two adjacent elements are not very different, see [12].

Over the fixed partition $\mathcal{T}_h$ we define the so-called broken Sobolev space with regularity given by the Sobolev index $s \geqslant 1$ as

$$H^s(\Omega, \mathcal{T}_h) \equiv \{v \in L^2(\Omega)\colon\ v|_{I_k} \in H^s(I_k)\ \forall\, I_k \in \mathcal{T}_h\}, \tag{3.1}$$

which plays an essential role in deriving the space semidiscretization, see [33]. Further, the approximate solution of (OPP) is constructed as a discontinuous piecewise polynomial function from the finite dimensional space associated with $\mathcal{T}_h$

$$S_h^p \equiv P_p(\Omega, \mathcal{T}_h) = \{v \in L^2(\Omega)\colon\ v|_{I_k} \in P_p(I_k)\ \forall\, I_k \in \mathcal{T}_h\}, \tag{3.2}$$

where $P_p(I_k)$ denotes the space of all polynomials of order less than or equal to p defined on I_k. Obviously, $S_h^p \subset H^1(\Omega, \mathcal{T}_h)$.

Since the functions $v \in S_h^p$ are discontinuous across partition nodes in general, we introduce $v(x_k^+) = \lim\limits_{\varepsilon \to 0+} v(x_k + \varepsilon)$ and $v(x_k^-) = \lim\limits_{\varepsilon \to 0+} v(x_k - \varepsilon)$. Then we can define the jump $[v(x_k)]$ and the mean value $\langle v(x_k)\rangle$ of v at inner partition nodes $x_k \in \Omega$ by

$$[v(x_k)] = v(x_k^-) - v(x_k^+), \quad \langle v(x_k)\rangle = \tfrac{1}{2}(v(x_k^-) + v(x_k^+)). \tag{3.3}$$

By convention, we also extend the definition (3.3) to both endpoints of Ω, i.e., $[v(x_0)] = -v(x_0^+)$, $\langle v(x_0)\rangle = v(x_0^+)$, $[v(x_N)] = v(x_N^-)$, and $\langle v(x_N)\rangle = v(x_N^-)$.

3.2. Spatial semidiscretization. Since (OPP) is defined in the space-time domain, the development of the numerical scheme consists of two consecutive phases—spatial semidiscretization and temporal discretization. Within the first phase we employ the DG framework and construct the solution from the space S_h^p with continuous time running (the so-called method of lines).

Based on standard techniques, we proceed similarly to [18] and introduce the semidiscrete variant of the differential part (2.26) as a bilinear form defined on $S_h^p \times S_h^p$ and decomposed into

$$\mathcal{D}_h(u, v) = a_h(u, v) + J_h(u, v) + b_h(u, v) + ((r + \lambda)u, v), \tag{3.4}$$

where

$$(3.5)\quad a_h(u,v) = \frac{\sigma^2}{2}\sum_{k=0}^{N-1}\int_{x_k}^{x_{k+1}} \frac{\partial u}{\partial x}\frac{\partial v}{\partial x}\,\mathrm{d}x - \frac{\sigma^2}{2}\sum_{k=0}^{N}\Big\langle\frac{\partial u}{\partial x}(x_k)\Big\rangle[v(x_k)] + \frac{\sigma^2}{2}\sum_{k=0}^{N}\Big\langle\frac{\partial v}{\partial x}(x_k)\Big\rangle[u(x_k)],$$

$$(3.6)\quad J_h(u,v) = \frac{\sigma^2 u(x_0^+)v(x_0^+)}{2h_1} + \frac{\sigma^2}{2}\sum_{k=1}^{N-1}\frac{[u(x_k)][v(x_k)]}{\max(h_k,h_{k+1})} + \frac{\sigma^2 u(x_N^-)v(x_N^-)}{2h_N},$$

$$(3.7)\quad b_h(u,v) = \Big(r-\lambda\kappa-\frac{\sigma^2}{2}\Big)\sum_{k=0}^{N-1}\int_{x_k}^{x_{k+1}} u\frac{\partial v}{\partial x}\,\mathrm{d}x + \sum_{k=0}^{N} H(u(x_k^-),u(x_k^+))[v(x_k)].$$

More precisely, the presented DG approach represents the so-called non-symmetric interior penalty Galerkin method ([33]), see the stabilization terms in (3.5) and the penalty terms (3.6), which also impose the Dirichlet boundary conditions. The essential role in the semidiscretization is played by the numerical flux H in (3.7), based on the concept of the upwinding (see [12]), which guarantees the propagation of the information through the partition nodes $x_k \in \overline{\Omega}$ in the positive or negative direction consistent with the sign of $\lambda\kappa + \frac{1}{2}\sigma^2 - r$ as

$$(3.8)\qquad H\Big(u(x_k^-),u(x_k^+)\Big) = \begin{cases} (\lambda\kappa+\frac{1}{2}\sigma^2-r)u(x_k^-) & \text{if } \lambda\kappa+\frac{1}{2}\sigma^2 \geqslant r,\\ (\lambda\kappa+\frac{1}{2}\sigma^2-r)u(x_k^+) & \text{if } \lambda\kappa+\frac{1}{2}\sigma^2 < r,\end{cases}$$

where the choice of $u(x_0^-)$ and $u(x_N^+)$ for boundary points $x_{\min}$ and $x_{\max}$ has to satisfy the prescribed Dirichlet boundary conditions (2.23) and (2.24), respectively.

Since there is a source term in the pricing equation (2.30) and in order to enforce the fulfillment of the boundary conditions, we introduce the linear form l_h balancing the boundary values in (3.5) and (3.6), i.e.,

$$(3.9)\quad l_h(v)(\hat{t}) = (\mathcal{R}(\hat{t}),v) + \frac{\sigma^2}{2}\Big(-\frac{\partial v}{\partial x}(x_0^+)u_L(\hat{t}) + \frac{\partial v}{\partial x}(x_N^-)u_U(\hat{t}) + \frac{u_L(\hat{t})v(x_0^+)}{h_1} + \frac{u_U(\hat{t})v(x_N^-)}{h_N}\Big).$$

In contrast to the BS framework, we also introduce the semidiscrete variant of (2.27), which formally remains the same as $L^2(\Omega)$-inner product with a convolution integral due to the inclusion $S_h^p \subset L^2(\Omega)$.

Now, we are ready to introduce the semidiscrete formulation of (OPP), which reads: Find $u_h \in H^1(0,T;S_h^p)$ such that the following conditions are satisfied:

$$\Big(\frac{\partial u_h(\hat{t})}{\partial \hat{t}}, v_h\Big) + \mathcal{D}_h(u_h(\hat{t}), v_h) = (\mathcal{I}_R(u_h(\hat{t})), v_h) + l_h(v_h)(\hat{t}) \quad \forall\, v_h \in S_h^p \quad \forall\, \hat{t} \in (0,T), \tag{3.10}$$

$$(u_h(0), v_h) = (\widehat{u}_0, v_h) \quad \forall\, v_h \in S_h^p. \tag{3.11}$$

The function u_h is the semidiscrete solution of (OPP), which is characterized as a solution of a system of ordinary differential equations (3.10) with the initial condition (3.11). Moreover, to ensure that $u_h(0) \in H^2(\Omega, \mathcal{T}_h)$ it is sufficient that $x = 0$ is a partition node of $\mathcal{T}_h$, cf. (2.9).

3.3. Temporal discretization. The second phase of the discretization aims at discretizing (OPP) on the time interval $[0,T]$ using the numerical scheme of a high accuracy in time and with no restrictive condition on the length of the time step. Let $0 = \hat{t}_0 < \hat{t}_1 < \ldots < \hat{t}_M = T$ be a partition of the interval $[0,T]$ with the constant time step $\tau = T/M$ (for simplicity) and denote by $u_h^m \in S_h^p$ the approximation of the solution $u_h(\hat{t})$ at time level $\hat{t}_m \in [0,T]$.

At first glance, one can directly propose to use the Crank-Nicolson method having the formal second order accuracy in time, i.e., (3.10) is discretized as

$$\begin{aligned}(u_h^{m+1}, v_h) + \frac{\tau}{2}\mathcal{D}_h(u_h^{m+1}, v_h) - \frac{\tau}{2}(\mathcal{I}_R(u_h^{m+1}), v_h) = (u_h^m, v_h) - \frac{\tau}{2}\mathcal{D}_h(u_h^m, v_h) \\ + \frac{\tau}{2}(\mathcal{I}_R(u_h^m), v_h) + \frac{\tau}{2}(l_h(v_h)(\hat{t}_{m+1}) + l_h(v_h)(\hat{t}_m)) \quad \forall\, v_h \in S_h^p.\end{aligned} \tag{3.12}$$

The equation (3.12) becomes a linear algebraic problem at each time level with a system matrix which is fully populated due to the nonlocal character of the integral term $(\mathcal{I}_R(\cdot), \cdot)$. This fact significantly increases the complexity of the solution procedure. On the other hand, it seems to be advantageous to evaluate the integral term in (3.12) only at stage u_h^m in order to decrease the density of the system matrix. However, the drawback of this approach is that the resulting accuracy of the scheme is only of the first order, which is not desirable.

Therefore, in what follows, we propose a scheme that retains the formal second order accuracy in time and leads to a sparse linear system of equations. The basic idea is to form the numerical scheme in two steps. Within the first step we use a semi-implicit Euler method to compute an approximation $\widetilde{u}_h^{m+1} \approx u_h^{m+1}$, i.e.,

$$(\widetilde{u}_h^{m+1}, v_h) + \tau\mathcal{D}_h(\widetilde{u}_h^{m+1}, v_h) = (u_h^m, v_h) + \tau(\mathcal{I}_R(u_h^m), v_h) + \tau l_h(v_h)(\hat{t}_{m+1}). \tag{3.13}$$

Then, in the second step we employ the scheme (3.12) using the stage $\widetilde{u}_h^{m+1}$ instead of u_h^{m+1} in the integral term. In this way we get a scheme that has the desired properties, see Subsection 3.5 and Section 4.

Apart from this, the crucial item of the solution procedure is the evaluation of the integral term. Commonly used direct approximations of this term are based on the standard quadrature methods (see e.g. [3] and [15]) which suffer from a high computational demandingness. To overcome this drawback it is possible to encompass a wavelet transform as in [28] or the fast Fourier transform (FFT), see also [2], [11] and [26]. Another alternative approach is presented in the forthcoming Subsection 3.4.

3.4. Integral term as an auxiliary problem. While the solutions of the differential part of (2.6) are frequently discussed in the literature and various methods have been proposed, relatively little can be found for the integral part of (2.6), see [23]. Moreover, this dissimilarity is much more evident for advanced option pricing techniques. In the following paragraphs we recall and modify the approach formulated for the first time in [7] which characterizes the function $\mathcal{I}_R(u)$ as a solution of a proper partial differential equation.

First we make change of variables $z = x+y$, then using (2.3) in the definition (2.27) leads to

$$\begin{aligned} \mathcal{I}_R(u)(x,\hat{t}) &= \frac{\lambda}{\sqrt{2\pi}\gamma} \int_{\mathbb{R}} u^e(z,\hat{t}) \exp\Big(-\frac{(z-x-\mu)^2}{2\gamma^2}\Big)\,\mathrm{d}z \\ &= \lambda \int_{\mathbb{R}} u^e(z,\hat{t}) \mathcal{F}(x+\mu-z, \tfrac{1}{2}\gamma^2)\,\mathrm{d}z, \end{aligned} \tag{3.14}$$

where $\mathcal{F}(x-z,\tilde{t})$ is the fundamental solution of the heat equation

$$\frac{\partial w}{\partial \tilde{t}} = \frac{\partial^2 w}{\partial x^2} \quad \text{in } \mathbb{R} \times (0, \tfrac{1}{2}\gamma^2) \tag{3.15}$$

with the artificial time $\tilde{t}$ corresponding to the variance of the jump process. Therefore, at any fixed time $\hat{t}$, one can easily view the function $\mathcal{I}_R(u)(x,\hat{t})/\lambda$ as a solution of the heat equation (3.15) with the initial condition $u^e(x,\hat{t})$, which is evaluated at $\tilde{t} = \frac{1}{2}\gamma^2$ and shifted by the amount μ, consequently.

Although the function $\mathcal{I}_R(u)$ has a support in $\mathbb{R}$, to speed up its evaluation process, it is advantageous to use a numerical scheme similar to that in Subsection 3.3, solving the equation (3.15) with the given initial data localized on the truncated domain Ω. This is feasible since the equation (3.15) is invariant with respect to the shift $x+\mu$. Therefore, one can argue that the spatial domain may remain the same as in the case of (OPP) instead of the shifted one $\Omega_\mu = (x_{\min}+\mu, x_{\max}+\mu)$. In contrast, we

use the shift $x+\mu$ only in the reformulation of the initial condition, which coincides with the restriction of $u^e(x,\hat{t})$ on Ω_μ.

Taking all the above mentioned into account means that at each time level $\hat{t}_m$ we solve the auxiliary initial-boundary value problem (AP) given by (3.15) restricted to Ω with the shifted initial condition

$$w(x,0) = u^e(x+\mu,\hat{t}_m), \quad x\in\Omega, \tag{3.16}$$

and artificially set boundary conditions corresponding to (2.10) and (2.11), i.e.,

$$w(x_{\min},\tilde{t}) = 0, \quad \frac{\partial w}{\partial x}(x_{\max},\tilde{t}) = \mathrm{e}^{x_{\max}+\mu}, \quad \tilde{t}>0 \quad \text{(call)}, \tag{3.17}$$

$$\frac{\partial w}{\partial x}(x_{\min},\tilde{t}) = -\mathrm{e}^{x_{\min}+\mu}, \quad w(x_{\max},\tilde{t}) = 0, \quad \tilde{t}>0 \quad \text{(put)}. \tag{3.18}$$

Then the exact solution of (AP) at $\tilde{t}=\frac{1}{2}\gamma^2$ defines the function

$$\widetilde{I}_R(u)(x,\hat{t}_m) = \lambda w(x,\tfrac{1}{2}\gamma^2), \quad x\in\Omega, \tag{3.19}$$

which is an approximation of $\mathcal{I}_R(u)$ on Ω in some sense, see Remark 3.2.

R e m a r k 3.1. The way of the definition of (AP) is justified from the financial point of view provided that $u^e|_{\Omega_\mu}$ is relevant to the option type (call or put). This is true, if $|\Omega|$ is sufficiently large compared to the value $|\mu|$ and the direction of the shift reflects the zero extension of the initial condition. More precisely, $\Omega\cap\Omega_\mu\neq\emptyset$ and $\mu\leqslant 0$ for calls or $\mu\geqslant 0$ for puts. In the case of opposite option types with the same shifts one can simply use the put-call parity (2.16) to transfer the prices from the above-mentioned options. Therefore, without loss of generality, in the rest of the paper it is possible to consider only call options with the positive shift ($\mu<0$) or put options with the negative one ($\mu>0$).

R e m a r k 3.2. The function $\widetilde{\mathcal{I}}_R(u)$ represents a reasonable approximation of $\mathcal{I}_R(u)$, since $\mathcal{I}_R(u)|_\Omega$ is given by the solution w of problem (3.15) restricted to Ω, where the boundary conditions (3.17) or (3.18) are replaced by the traces of w on the boundary of Ω. It can be assumed for the domain Ω large enough that the boundary conditions defining problem (AP) are close to the original traces of w on the boundary of Ω. The approximation of $\mathcal{I}_R(u)$ by $\widetilde{\mathcal{I}}_R(u)$ then follows from the stability with respect to the boundary condition for the heat equation.

Since the spatial domain is identical to the one considered in (OPP), we can here simply use the same function spaces and forms and schemes similar to those in Subsections 3.1–3.3. Analogously to (3.10) the semidiscrete solution of (AP) satisfies

$$\Big(\frac{\partial w_h(\tilde{t})}{\partial\tilde{t}}, v_h\Big) + \mathcal{A}_h(w_h(\tilde{t}),v_h) = l_h^*(v_h) \quad \forall\, v_h\in S_h^p, \quad \forall\,\tilde{t}\in(0,\tfrac{1}{2}\gamma^2), \tag{3.20}$$

where

$$\mathcal{A}_h(w,v) = \sum_{k=0}^{N-1} \int_{x_k}^{x_{k+1}} \frac{\partial w}{\partial x}\frac{\partial v}{\partial x}\,\mathrm{d}x - \sum_{k=0}^{N-1} \Big\langle \frac{\partial w}{\partial x}(x_k) \Big\rangle [v(x_k)] + \sum_{k=0}^{N-1} \Big\langle \frac{\partial v}{\partial x}(x_k) \Big\rangle [w(x_k)] + \frac{w(x_0^+)v(x_0^+)}{h_1} + \sum_{k=1}^{N-1} \frac{[w(x_k)][v(x_k)]}{\max(h_k, h_{k+1})}, \tag{3.21}$$

$$l_h^*(v) = \mathrm{e}^{x_{\max}+\mu} v(x_N^-). \tag{3.22}$$

Without loss of generality, the forms (3.21) and (3.22) represent the case of call options. Their generalization for put options is straightforward using (3.18) and it is left to the reader.

Further, in a way similar to that in (3.12), we introduce the discrete solution of (AP) as the function $w_h^{m^*} \approx w_h(\tilde{t}_{m^*})$ at time levels $0 = \tilde{t}_0 < \tilde{t}_1 < \ldots < \tilde{t}_{M^*} = \frac{1}{2}\gamma^2$ with constant time step τ^* as

$$(w_h^{m^*+1}, v_h) + \frac{\tau^*}{2}\mathcal{A}_h(w_h^{m^*+1}, v_h) = (w_h^{m^*}, v_h) - \frac{\tau^*}{2}\mathcal{A}_h(w_h^{m^*}, v_h) + \tau^* l_h^*(v_h) \quad \forall\, v_h \in S_h^p,\ m^* = 0, 1, \ldots, M^* - 1. \tag{3.23}$$

Finally, note that taking the time step τ^* in (AP) proportional to τ in (OPP), i.e., there exists a constant $\overline{C} > 0$ such that $\tau^* \leqslant \overline{C}\tau$, does not violate the formal second order accuracy of the resulting numerical scheme, see Section 4.

3.5. Numerical scheme and its algebraic representation. Now we are ready to introduce the concept of a discrete solution that is computed by a numerical scheme based on a combination of the semi-implicit Euler method and the Crank-Nicolson scheme, where the integral terms are evaluated as the approximate solutions of the auxiliary initial-boundary value problems.

Definition 3.1. The discrete setting of (OPP) reads: Find $u_h^{m+1}, \widetilde{u}_h^{m+1} \in S_h^p$, $m = 0, \ldots, M-1$ such that the following conditions are satisfied:

$$(\widetilde{u}_h^{m+1}, v_h) + \tau \mathcal{D}_h(\widetilde{u}_h^{m+1}, v_h) = (u_h^m, v_h) + \tau(\widetilde{\mathcal{I}}_h(u_h^m), v_h) + \tau l_h(v_h)(\hat{t}_{m+1}) \quad \forall\, v_h \in S_h^p, \tag{3.24}$$

$$(u_h^{m+1}, v_h) + \tfrac{1}{2}\tau \mathcal{D}_h(u_h^{m+1}, v_h) - \tfrac{1}{2}\tau(\widetilde{\mathcal{I}}_h(\widetilde{u}_h^{m+1}), v_h) = (u_h^m, v_h) - \tfrac{1}{2}\tau \mathcal{D}_h(u_h^m, v_h) + \tfrac{1}{2}\tau(\widetilde{\mathcal{I}}_h(u_h^m), v_h) + \tfrac{1}{2}\tau(l_h(v_h)(\hat{t}_{m+1}) + l_h(v_h)(\hat{t}_m)) \quad \forall\, v_h \in S_h^p, \tag{3.25}$$

$$u_h^0 \text{ is the } S_h^p\text{-approximation of } \widehat{u}_0, \tag{3.26}$$

where $\widetilde{\mathcal{I}}_h(u_h^m) = \lambda w_h^{M^*}$ and $\widetilde{\mathcal{I}}_h(\widetilde{u}_h^{m+1}) = \lambda \widetilde{w}_h^{M^*}$ are scaled solutions of (AP) given by the scheme (3.23) with the shifted starting data, defined by projections

$$(w_h^0(x), v_h) = (u_h^{m,e}(x+\mu), v_h) \quad \forall\, v_h \in S_h^p, \tag{3.27}$$

$$(\widetilde{w}_h^0(x), v_h) = (\widetilde{u}_h^{m+1,e}(x+\mu), v_h) \quad \forall\, v_h \in S_h^p, \tag{3.28}$$

and $u_h^{m,e}$, $\widetilde{u}_h^{m+1,e}$ stand for the zero extension of functions u_h^m, $\widetilde{u}_h^{m+1}$, respectively.

Since the discrete problems (3.23)–(3.25) are equivalent to the systems of linear algebraic equations at the corresponding time levels, we express them in matrix forms as follows. Let $\mathcal{B} = \{\varphi_j\}_{j=1}^{\mathrm{DOF}}$ denote the basis of the space S_h^p with dimension $\mathrm{DOF} = N(p+1)$. Then the discrete solution of (OPP) at each time level $\hat{t}_m \in [0,T]$ can be written in the form $u_h^m = \sum\limits_{j=1}^{\mathrm{DOF}} \alpha_j^m \varphi_j$ and identified with the coefficient vector $U_m = \{\alpha_j^m\}_{j=1}^{\mathrm{DOF}}$ with respect to the basis $\mathcal{B}$. Analogously, the discrete solution of (AP) at each time level $\tilde{t}_{m^*} \in [0, \frac{1}{2}\gamma^2]$ can be seen as $w_h^{m^*} = \sum\limits_{j=1}^{\mathrm{DOF}} \beta_j^{m^*} \varphi_j$ and the vector $W_{m^*} = \{\beta_j^{m^*}\}_{j=1}^{\mathrm{DOF}}$.

Then, (3.23) for (AP) reads

$$\Big(\mathbf{M} + \frac{\tau^*}{2}\mathbf{A}\Big) W_{m^*+1} = \Big(\mathbf{M} - \frac{\tau^*}{2}\mathbf{A}\Big) W_{m^*} + \tau^* G \tag{3.29}$$

and (3.24)–(3.25) for (OPP) are rewritten as

$$(\mathbf{M} + \tau\mathbf{D})\widetilde{U}_{m+1} = \mathbf{M}U_m + \tau\lambda\mathbf{M}W_{M^*} + \tau F_{m+1}, \tag{3.30}$$

$$\begin{aligned}\Big(\mathbf{M} + \frac{\tau}{2}\mathbf{D}\Big) U_{m+1} = {} & \Big(\mathbf{M} - \frac{\tau}{2}\mathbf{D}\Big) U_m + \frac{\tau\lambda}{2}\mathbf{M}(\widetilde{W}_{M^*} + W_{M^*}) \\ & + \frac{\tau}{2}(F_{m+1} + F_m),\end{aligned} \tag{3.31}$$

where W_{M^*} and $\widetilde{W}_{M^*}$ are given by (3.29) with the initial vectors W_0 and $\widetilde{W}_0$ arising from U_m and $\widetilde{U}_{m+1}$ by (3.27) and (3.28), respectively.

The system matrices in (3.29)–(3.31) are compositions of the mass matrix $\mathbf{M}$ and the matrix $\mathbf{A}$ arising from the bilinear form $\mathcal{A}_h$ or the matrix $\mathbf{D}$ from the form $\mathcal{D}_h$, defined as

$$\mathbf{M} = \{(\varphi_j, \varphi_i)\}_{i,j=1}^{\mathrm{DOF}}, \quad \mathbf{A} = \{\mathcal{A}_h(\varphi_j, \varphi_i)\}_{i,j=1}^{\mathrm{DOF}}, \quad \mathbf{D} = \{\mathcal{D}_h(\varphi_j, \varphi_i)\}_{i,j=1}^{\mathrm{DOF}}. \tag{3.32}$$

The right-hand sides of the linear problems above contain also vectors resulting from the prescribed boundary conditions, i.e.,

$$G = \{l_h^*(\varphi_j)\}_{j=1}^{\mathrm{DOF}},\ F_m = \{l_h(\varphi_j)(\hat{t}_m)\}_{j=1}^{\mathrm{DOF}},\ F_{m+1} = \{l_h(\varphi_j)(\hat{t}_{m+1})\}_{j=1}^{\mathrm{DOF}}. \tag{3.33}$$

R e m a r k 3.3. The shift in projections (3.27) and (3.28) is simply defined on equally spaced partitions $\mathcal{T}_h$ provided that $x_{\min} - \mu$ (for calls) or $x_{\max} - \mu$ (for puts) are partition nodes. Then, it is enough to shift only components of vectors U_m, $\widetilde{U}_{m+1}$ and the rest of them is defined as zeros.

Since $\mathcal{A}_h(w,v) \neq \mathcal{A}_h(v,w)$, $\mathcal{D}_h(u,v) \neq \mathcal{D}_h(v,u)$ and the supports of the basis functions $\{\varphi_j\}_{j=1}^{\mathrm{DOF}}$ are small, the system matrices are non-symmetric and sparse with a block structure. Therefore, we use a suitable iterative solver in practical computations, see Subsection 5.1. The obtained solution vector uniquely determines the approximate solution at each time level, whose existence and uniqueness correspond with the solvability of these linear systems, see Remark 4.1 in Section 4.

Finally, for the sake of clarity, the whole numerical procedure for valuing of European-style options under the Merton model can be summarized into the following processes:

(1) set the initial state u_h^0 according to the type of option (2.9)

`for` $m = 0$ `to` $M - 1$ `do`

(2) set the shifted initial state w_h^0 arising from u_h^m by projection (3.27)
(3) solve (AP) by scheme (3.29) and evaluate $\widetilde{\mathcal{I}}_h(u_h^m) = \lambda w_h^{M^*}$
(4) solve (OPP) by scheme (3.30) to obtain $\widetilde{u}_h^{m+1}$
(5) set the shifted initial state $\widetilde{w}_h^0$ arising from $\widetilde{u}_h^{m+1}$ by projection (3.28)
(6) solve (AP) by scheme (3.29) and evaluate $\widetilde{\mathcal{I}}_h(\widetilde{u}_h^{m+1}) = \lambda \widetilde{w}_h^{M^*}$
(7) solve (OPP) by scheme (3.31) to obtain u_h^{m+1}

`endfor`

4. A priori error estimates

The goal of this section is to present an a priori error analysis of the method set up in Definition 3.1 with respect to the chosen discretization parameters h, p, and τ. We neglect the effect of the truncation of the computational domain from $\mathbb{R}$ to Ω in this analysis and we just assume that the domain Ω is taken large enough so that all approximations coming from this truncation are negligible. To this end, we investigate the error between the discrete solution u_h and truncated solution u_R only. The error between the true solution $\widehat{u}$ and u_R is described by (2.15). For the detailed discussion of the effect of the truncation on the numerical results see e.g. [9].

Let us assume for the purpose of the convergence analysis that the solution u_R of problem (2.12) satisfies

$$u_R \in W^{3,\infty}(0,T,L^2(\Omega)) \cap W^{1,\infty}(0,T,H^{p+1}(\Omega)). \tag{4.1}$$

Moreover, the sufficient smoothness of the solution w of problem (AP) is needed for the analysis of the complete problem as well. Essentially, the regularity of w is inherited from the smoothness of its initial condition, i.e., from $u_R(\hat{t})$, if the compatibility conditions relating the initial condition and the boundary conditions are satisfied. For the original problem without truncation to Ω such compatibility assumptions are satisfied trivially. A different situation occurs for the truncated problem, where the boundary conditions are determined from the asymptotic behavior of the solution, see (3.17) and (3.18). On the other hand, these artificial boundary conditions are close to the correct ones, if the domain Ω is taken large enough. Therefore the solution w is close to the smooth one, see Remark 3.2. To this end, we simplify the next considerations by the assumption that the solution w satisfies regularity (4.1) too.

According to [14] we define the energy norm corresponding to the form $\mathcal{D}_h(\cdot,\cdot)$ as

$$\begin{aligned}(4.2)\qquad |\!|\!| u_h |\!|\!|^2 = \frac{\sigma^2}{2}\sum_{k=1}^{N}\Big\|\frac{\partial u_h}{\partial x}\Big\|^2_{L^2(I_k)} + (r+\lambda)\|u_h\|^2 + \frac{\sigma^2}{2}J_h(u_h,u_h)\\ + \frac{1}{2}\Big|r-\lambda\kappa-\frac{\sigma^2}{2}\Big|\sum_{k=0}^{N}[u_h(x_k)]^2.\end{aligned}$$

A generic constant $C>0$ will be used in the following analysis, where the constant C can depend on the data of the problem (e.g. λ, r, T, etc.), on the constant describing the quasi-uniformity of the mesh, on the degree of the polynomial approximation p, on the constant $\overline{C}>0$ binding step sizes τ^* and τ and on the norms $\|u_R\|_{W^{3,\infty}(0,T,L^2(\Omega))}$, $\|u_R\|_{W^{1,\infty}(0,T,H^{p+1}(\Omega))}$, but the constant C is independent of the mesh size h and step size τ.

Lemma 4.1. *There exists a constants $C>0$ such that*

$$(4.3)\qquad \mathcal{D}_h(u_h,v_h) \leqslant C|\!|\!| u_h |\!|\!| |\!|\!| v_h |\!|\!| \quad \forall\, u_h, v_h \in S_h^p,$$

$$(4.4)\qquad \mathcal{D}_h(u_h,u_h) = |\!|\!| u_h |\!|\!|^2 \quad \forall\, u_h \in S_h^p.$$

Moreover, we define the Ritz projection $R_h\colon H^2(\Omega,\mathcal{T}_h)\to S_h^p$ such that

$$(4.5)\qquad \mathcal{D}_h(R_hu-u,v_h)=0 \quad \forall\, u\in H^2(\Omega,\mathcal{T}_h), v_h\in S_h^p.$$

Then there exists a constant $C>0$ such that

$$(4.6)\qquad \|R_hu-u\| \leqslant Ch^p|u|_{H^{p+1}(\Omega)} \quad \forall\, u\in H^{p+1}(\Omega).$$

P r o o f. The proof of (4.3)–(4.4) and (4.6) can be found in [14]. The existence and uniqueness of the Ritz projection R_h follow from (4.3)–(4.4) and the Lax-Milgram lemma. □

R e m a r k 4.1. According to Lemma 4.1, the matrices $\mathbf{M} + \tau\mathbf{D}$ and $\mathbf{M} + \frac{1}{2}\tau\mathbf{D}$ are positive definite. This yields the existence and uniqueness of the discrete solution of problems (3.24) and (3.25).

Lemma 4.2. *Let $\tau^* \leqslant \overline{C}\tau$. Then there exists a constant $C > 0$ such that*

$$(\widetilde{\mathcal{I}}_h(u_h), v_h) - (\mathcal{I}_R(u_R), v_h) \leqslant C(h^p + \tau^2 + \|u_h - u_R\|)\|v_h\| \quad \forall\, u_h, v_h \in S_h^p. \tag{4.7}$$

P r o o f. Since $\|\mathcal{I}_R(u_R) - \widetilde{\mathcal{I}}_h(u_h)\| = \lambda\|w(\frac{1}{2}\gamma^2) - w_h^{M^*}\|$, where w is the solution of problem (AP) and w_h is the solution given by (3.23), it is sufficient to estimate $w(\frac{1}{2}\gamma^2) - w_h^{M^*}$ only. The estimate

$$\|w(\tfrac{1}{2}\gamma^2) - w_h^{M^*}\| \leqslant C(h^p + (\tau^*)^2 + \|u_h - u_R\|) \tag{4.8}$$

can be derived by the standard a priori error estimates technique for the heat equation discretized by the discontinuous Galerkin method in space and by the Crank-Nicolson method in time, see e.g. [12] and [35]. Finally, the estimate (4.7) follows from the assumption $\tau^* \leqslant C\tau$. □

Lemma 4.3. *Let $v_h \in S_h^p$. Then there exists a constant $C > 0$ such that*

$$\Big(\frac{\tau}{2}\frac{\partial u_R}{\partial \hat{t}}(\hat{t}_{m+1}) + \frac{\tau}{2}\frac{\partial u_R}{\partial \hat{t}}(\hat{t}_m) - u_R(\hat{t}_{m+1}) + u_R(\hat{t}_m), v_h\Big) \leqslant C\tau^3\|v_h\|, \tag{4.9}$$

$$\Big(\tau\frac{\partial u_R}{\partial \hat{t}}(\hat{t}_{m+1}) - u_R(\hat{t}_{m+1}) + u_R(\hat{t}_m), v_h\Big) \leqslant C\tau^2\|v_h\|, \tag{4.10}$$

$$((R_h u_R - u_R)(\hat{t}_{m+1}) - (R_h u_R - u_R)(\hat{t}_m), v_h) \leqslant C\tau h^p\|v_h\|. \tag{4.11}$$

P r o o f. The proof can be done similarly to [13]. □

We are ready to formulate the main convergence theorem.

Theorem 4.1. *Let u_R be the solution of problem* (2.12) *satisfying* (4.1) *and let $\{u_h^m\}_{m=1}^M \subset S_h^p$ be the discrete solutions given by* (3.24) *and* (3.25)*, where $\tau^* \leqslant \overline{C}\tau$. Then there exist constants $c^*, C > 0$ such that $\tau \leqslant c^*$ implies*

$$\max_{m=1,\dots,M} \|u_h^m - u_R(\hat{t}_m)\| \leqslant C(h^p + \tau^2). \tag{4.12}$$

P r o o f. We divide the error setting $u_h^m - u_R(\hat{t}_m) = \xi^m + \eta^m$, where $\xi^m = u_h^m - R_h u_R(\hat{t}_m) \in S_h^p$ and $\eta^m = R_h u_R(\hat{t}_m) - u_R(\hat{t}_m)$. Since $\|\eta^m\|$ can be estimated by Lemma 4.1, it is sufficient to estimate ξ^m only. The term ξ^{m+1} satisfies the error equation

$$
\begin{aligned}
(4.13)\quad (\xi^{m+1} - \xi^m, v_h) + \frac{\tau}{2}\mathcal{D}_h(\xi^{m+1} + \xi^m, v_h) &= \frac{\tau}{2}(\widetilde{\mathcal{I}}_h(\widetilde{u}_h^{m+1}) - \widetilde{\mathcal{I}}_R(u_R(\hat{t}_{m+1})), v_h) \\
&+ \frac{\tau}{2}(\widetilde{\mathcal{I}}_h(u_h^m) - \widetilde{\mathcal{I}}_R(u_R(\hat{t}_m)), v_h) - (\eta^{m+1} - \eta^m, v_h) \\
&+ \Big(\frac{\tau}{2}\frac{\partial u_R}{\partial \hat{t}}(\hat{t}_{m+1}) + \frac{\tau}{2}\frac{\partial u_R}{\partial \hat{t}}(\hat{t}_m) - u_R(\hat{t}_{m+1}) + u_R(\hat{t}_m), v_h\Big).
\end{aligned}
$$

Applying Lemma 4.2 and Lemma 4.3, we get

$$
\begin{aligned}
(4.14)\qquad (\xi^{m+1} - \xi^m, v_h) + \frac{\tau}{2}\mathcal{D}_h(\xi^{m+1} + \xi^m, v_h) \\
\leqslant C\tau(h^p + \tau^2 + \|\widetilde{u}_h^{m+1} - u_R(\hat{t}_{m+1})\| + \|u_h^m - u_R(\hat{t}_m)\|)\|v_h\|,
\end{aligned}
$$

where $\|u_h^m - u_R(\hat{t}_m)\| \leqslant Ch^p + \|\xi^m\|$. The next step is the estimation of the norm $\|\widetilde{u}_h^{m+1} - u_R(\hat{t}_{m+1})\|$. We again divide the error as $\widetilde{u}_h^{m+1} - u_R(\hat{t}_{m+1}) = \widetilde{\xi}^{m+1} + \eta^{m+1}$, where $\widetilde{\xi}^{m+1} = \widetilde{u}_h^{m+1} - R_h u_R(\hat{t}_{m+1}) \in S_h^p$. Then the term $\widetilde{\xi}^{m+1}$ satisfies

$$
\begin{aligned}
(4.15)\qquad (\widetilde{\xi}^{m+1} - \xi^m, v_h) + \tau\mathcal{D}_h(\widetilde{\xi}^{m+1}, v_h) &= \tau(\widetilde{\mathcal{I}}_h(u_h^m) - \widetilde{\mathcal{I}}_R(u_R(\hat{t}_m)), v_h) \\
&- (\eta^{m+1} - \eta^m, v_h) + \Big(\tau\frac{\partial u_R}{\partial \hat{t}}(\hat{t}_{m+1}) - u_R(\hat{t}_{m+1}) + u_R(\hat{t}_m), v_h\Big).
\end{aligned}
$$

Applying Lemma 4.2 and Lemma 4.3, we get

$$
(4.16)\qquad (\widetilde{\xi}^{m+1} - \xi^m, v_h) + \tau\mathcal{D}_h(\widetilde{\xi}^{m+1}, v_h) \leqslant C\tau(h^p + \tau + \|\xi^m\|)\|v_h\|.
$$

Setting $v_h = \widetilde{\xi}^{m+1}$ in (4.16) and applying the positivity of the form $\mathcal{D}_h(\cdot,\cdot)$, see Lemma 4.1, we get

$$
(4.17)\qquad \|\widetilde{\xi}^{m+1}\|^2 \leqslant \|\xi^m\|\|\widetilde{\xi}^{m+1}\| + C\tau(h^p + \tau + \|\xi^m\|)\|\widetilde{\xi}^{m+1}\|.
$$

Dividing the relation (4.17) by $\|\widetilde{\xi}^{m+1}\|$, we get

$$
(4.18)\qquad \|\widetilde{\xi}^{m+1}\| \leqslant C\|\xi^m\| + C(h^p + \tau^2).
$$

Now, we can insert the estimate (4.18) into (4.14) to obtain

$$
(4.19)\qquad (\xi^{m+1} - \xi^m, v_h) + \frac{\tau}{2}\mathcal{D}_h(\xi^{m+1} + \xi^m, v_h) \leqslant C\tau(h^p + \tau^2 + \|\xi^m\|)\|v_h\|.
$$

Setting $v_h = \xi^{m+1} + \xi^m$ and applying the positivity of the form $\mathcal{D}_h(\cdot,\cdot)$, see Lemma 4.1, and Young's inequality, we get

$$\begin{aligned}(4.20)\qquad \|\xi^{m+1}\|^2 - \|\xi^m\|^2 &\leqslant C\tau(h^p + \tau^2 + \|\xi^m\|)(\|\xi^{m+1}\| + \|\xi^m\|)\\ &\leqslant \tau\|\xi^{m+1}\|^2 + \tau\|\xi^m\|^2 + C\tau(h^{2p} + \tau^4 + \|\xi^m\|^2).\end{aligned}$$

Finally, the desired estimate (4.12) follows from the discrete Gronwall's lemma under the assumption $\tau \leqslant \frac{1}{2} = c^*$. □

R e m a r k 4.2. The assumption $\tau \leqslant c^*$ is not necessary for deriving the estimate (4.12). It just simplifies the use of the discrete Gronwall's lemma. A modification of the technique of the proof without this assumption can be found in [36].

R e m a r k 4.3. The order of convergence in the L^2-norm derived in Theorem 4.1 is $\mathcal{O}(h^p + \tau^2)$, although the expected order for approximation with polynomials of degree p is $\mathcal{O}(h^{p+1} + \tau^2)$. This suboptimality is caused by the non-symmetric DG discretization, where only the order $\mathcal{O}(h^p)$ is proved, see e.g. [12]. Nevertheless, the optimal order is often observed in computations, if the order p is an odd number. The general proof of the optimal order of convergence for the non-symmetric DG discretization with odd polynomial degree p is an open problem in the DG analysis.

5. Numerical experiments

In this section, we present numerical experiments on the standard benchmark of the Merton model in order to illustrate the usage and convergence of the proposed numerical scheme. Initially, we present the model parameters and mention some implementation aspects. Then, we numerically price European options with respect to the different parameters h and τ as well as the polynomial orders of approximation p and the length of the computational domain $|\Omega|$. From the practical point of view we evaluate the options at several underlying nodes and compare these values to the reference and analytical ones. Next, we investigate the convergence property and orders of the discretization scheme. Finally, we append a simple sensitivity measurement to outline one of the possible ways of further analysis.

5.1. Parameter settings. The numerical benchmark is performed on the reference data from [11] and [26], where the European call and put option prices under the Merton model are evaluated using a finite difference method. More specifically, the paper [11] presents a fixed point iteration scheme with incorporated FFT method for the rapid evaluation of the integral term. In [26], authors construct a numerical

method, where the composite trapezoidal rule approximates the integral term on the bounded region and again FFT algorithm is employed.

In all cases, we consider a call option with the data

$$T = 0.25,\ \mathcal{K} = 100,\ \sigma = 0.15,\ r = 0.05,\ \lambda = 0.1,\ \mu = -0.90,\ \gamma = 0.45, \tag{5.1}$$

which are the representatives of parameter values of practical significance. From the financial point of view, we can expect that σ, r, λ, $\gamma \in (0.01, 1)$ and $|\mu| \leqslant 1$.

The whole implementation of the proposed numerical scheme is done in the solver freefem++, for more details see [17]. Taking the properties of matrices (3.32) into account, GMRES solver is employed and it uses the solution from the previous time level as an initial guess. Since these linear systems are relatively small (i.e., DOF $< 10^4$), no preconditioner is needed.

According to the localization error (2.15), the actual convergence properties of the scheme (3.23)–(3.25) cannot be observed near the boundary $\partial\Omega$. Therefore, we investigate pricing errors due to localization and spatial and temporal discretizations on a zone of financial interest $\Omega^* \subset \Omega$, that is appropriately located with respect to $\partial\Omega$, for more details, see [15]. In order to indicate the convergence of option prices and to determine the orders of convergence, we consider piecewise linear ($p = 1$) and quadratic ($p = 2$) approximations on the uniformly partitioned (consecutively refined) grids with halving the number of time steps.

5.2. Point-wise errors. Within the first part of a numerical verification of the scheme derived, we analyze its point-wise behaviour. This approach is the most common from the practical point of view, when options are numerically priced.

At the beginning, we start with the proper setting of the length of the computational domain $\Omega = (-x_{\max}, x_{\max})$ within the localization errors and investigate the effect of the localization in Merton-type models. Therefore, we compute the numerical solutions on a sequence of the consecutively expanding grids with fixed (sufficiently small) spatial and temporal parameters $h = 10^{-3}$ and $\tau = T/800$ that suppress the influence of these discretizations on the resulting errors. The zone of financial interest is set in consistency with the experimental study from [15] as $\Omega^* = [\ln(0.8), \ln(1.2)]$ to cover interval $[80, 120]$ in the original underlying asset prices.

The comparative results are evaluated at underlying prices $S_{\text{ref}} \in \{90, 100, 110\}$ at time state $\hat{t} = T$, see Table 1. The results obtained are associated with the analytical values, since the problem (2.4) has an analytical solution given by Merton's formula [30].

Assuming constant model parameters, under the Merton model the European option price can be expressed as an infinite sum

$$V_{\mathrm{Mer}}(S,t) = \sum_{n=0}^{\infty} \frac{\mathrm{e}^{-\lambda'(T-t)}(\lambda'(T-t))^n}{n!} V_{\mathrm{BS}}(S,t,\mathcal{K},\sigma_n,r_n), \tag{5.2}$$

where

$$\lambda' = \lambda(\kappa+1), \quad \sigma_n^2 = \sigma^2 + \frac{n\gamma^2}{T-t}, \quad r_n = r - \lambda\kappa + \frac{n\ln(\kappa+1)}{T-t}$$

and V_{BS} is the classical Black-Scholes formula [16]

$$V_{\mathrm{BS}}(S,t,\mathcal{K},\sigma,r) = \begin{cases} S\Phi(d_1) - \mathcal{K}\mathrm{e}^{-r(T-t)}\Phi(d_2), & \text{for a call,} \\ -S\Phi(-d_1) + \mathcal{K}\mathrm{e}^{-r(T-t)}\Phi(-d_2), & \text{for a put} \end{cases} \tag{5.3}$$

with

$$d_1 = \frac{\ln(S/\mathcal{K}) + (r + \frac{1}{2}\sigma^2)(T-t)}{\sigma\sqrt{T-t}}, \quad d_2 = d_1 - \sigma\sqrt{T-t}.$$

For the purpose of the comparison it is sufficient to evaluate only the first five terms in the sum (5.2) to provide accuracy of 6 digits after the decimal point.

Moreover, in Table 1, we add errors in the discrete l^∞-norm that are very important in financial engineering as the worst-case pricing scenario, i.e.,

$$e_{h,\infty}^M(P_p) = \max_{x_i \in \mathcal{T}_h} |\mathcal{K}u_h^M(x_i) - V_{\mathrm{Mer}}(\mathcal{K}\mathrm{e}^{x_i}, 0)|, \tag{5.4}$$

where x_i are all nodes lying in the zone of financial interest, associated with degrees of freedom, and V_{Mer} is given by (5.2).

$\mathrm{DG}(P_p)$	$x_{\max}$	$S=90$	$S=100$	$S=110$	$e_{h,\infty}^M(P_p)$
	0.5	0.892979	5.022568	13.644522	1.8335e − 00
	1.0	0.552374	4.442992	12.740900	2.2623e − 01
	1.5	0.528353	4.393021	12.647550	1.2433e − 02
$p=1$	2.0	0.527655	4.391220	12.643473	2.5531e − 04
	2.5	0.527648	4.391198	12.643412	6.3301e − 05
	3.0	0.527648	4.391198	12.643412	6.3301e − 05
$p=2$	3.0	0.527637	4.391147	12.643406	9.5689e − 05
analytical value [30]		0.527638	4.391246	12.643406	—

Table 1. Comparison of the approximate option values with the analytical results at three reference nodes for different lengths of the computational domain Ω.

From the results listed in Table 1, one can conclude that the numerical option prices are of higher accuracy as the length of the computational domain Ω increases

with respect to the fixed zone of financial interest Ω^*. These observations are in a quite good agreement with the theoretical estimates of localization errors (2.15). Further, the last column in Table 1 indicates for this experimental study that the restriction to the computational domain $\Omega = (-3, 3)$ is sufficient and taking another larger domains does not improve the results significantly, if the time-space grid is no longer finer. Therefore, for the forthcoming experiments, we always assume $\Omega = (-3, 3)$.

The next set of experiments investigates the behaviour of point-wise errors with respect to the discretization parameters h and τ. The time-space grids are designed to ensure the highest consistency with refereed experiments from [11] and [26].

The results are recorded in Table 2, which has the format similar to that in the preceding experiments. One can easily observe that numerical option prices are of higher accuracy as the time-space mesh is finer. The last column of this table indicates the ratio of the error in the l^∞-norm to the error in the previous computational domain. The level of the finest setting corresponds with reference values from [11] and [26]. From this point of view the results obtained are quite comparable with reference ones and are also close to the analytical values with almost 5 digits of accuracy. The results thus meet the expectations of financial practitioners.

DG(P_p)	M	N	$S = 90$	$S = 100$	$S = 110$	$e^M_{h,\infty}(P_p)$	ratio
	25	128	0.531863	4.349031	12.609051	1.0996e − 01	—
	50	256	0.535127	4.380516	12.636871	2.8337e − 02	3.881
	100	512	0.524578	4.388452	12.642699	7.0826e − 03	4.001
$p = 1$	200	1024	0.526917	4.390482	12.643580	1.7872e − 03	3.963
	400	2048	0.527479	4.391035	12.643508	4.5708e − 04	3.910
	800	4096	0.527608	4.391192	12.643380	1.2380e − 04	3.692
	25	128	0.529053	4.381145	12.646109	1.0739e − 02	—
	50	256	0.527328	4.388380	12.644153	3.0157e − 03	3.561
	100	512	0.527562	4.390356	12.643588	8.8569e − 04	3.405
$p = 2$	200	1024	0.527619	4.390891	12.643447	3.5569e − 04	2.490
	400	2048	0.527633	4.391082	12.643414	1.6569e − 04	2.148
	800	4096	0.527637	4.391181	12.643407	1.4244e − 04	1.163
reference value [11]			0.527637	4.391243	12.643404	—	—
reference value [26]			0.527636	4.391211	12.643397	—	—
analytical value [30]			0.527638	4.391246	12.643406	—	—

Table 2. Comparison of the approximate option values with the reference and analytical values at three reference nodes for different mesh sizes, time steps and polynomial orders.

5.3. L^2-convergence. The second part aims at determining the experimental orders of convergence (EOC) with respect to the L^2-norm. The convergence property is investigated on a zone of financial interest $\Omega^* = (-3, \ln 2)$ that covers a domain up to the double strike price $\mathcal{K}$ and is sufficient from a practical standpoint.

At the final state $\hat{t} = T$, for piecewise linear (P_1) and quadratic (P_2) polynomial approximations, we compute the relative errors

$$e^M_{h,2}(P_p) = \frac{\|\mathcal{K}u^M_h(x) - V_{\mathrm{Mer}}(\mathcal{K}\mathrm{e}^x, 0)\|_{L^2(\Omega^*)}}{\|V_{\mathrm{Mer}}(\mathcal{K}\mathrm{e}^x, 0)\|_{L^2(\Omega^*)}}, \quad p = 1, 2. \tag{5.5}$$

According to a priori error estimates, the errors (5.5) behave as $\mathcal{O}(h^p+\tau^2)$, see Theorem 4.1, or $\mathcal{O}(h^{p+1} + \tau^2)$, see Remark 4.3. To this end we can expect the second order of convergence for $p = 1$ and $p = 2$. Considering a sequence of meshes with halving $h = |\Omega|/N$ and $\tau = T/M$ parameters, the experimental order of convergence is defined by

$$\mathrm{EOC} = \log_2(e^M_{h,2}(P_p)/e^{2M}_{h/2,2}(P_p)), \quad p = 1, 2. \tag{5.6}$$

In contrast to [15], we would like to illustrate also the robustness of the scheme with respect to the model parameters which determines the convection-diffusion character of the pricing equation (2.21).

The setting (5.1) corresponds approximately to the ratio $\frac{\text{convection}}{\text{diffusion}} \sim 10$, see the differential part (2.7). To obtain the convection dominated problem within the parameters of practical significance, we further consider a less volatile market with $\sigma = 0.01$ that is close to the pure jump model. The rest of parameters in (5.1) remains unchanged. This case leads to the problem with ratio $\frac{\text{convection}}{\text{diffusion}} \sim 10^3$, which is difficult to solve without stabilization mechanism by finite element methods as in [15] or without upwinding techniques in finite difference schemes as in [26]. This is not a case of the presented scheme that already has incorporated the upwind to be sufficiently robust for the convection dominated problems, see (3.7)–(3.8).

The results of the experimental analysis for both values of σ are recorded in Table 3. This table is divided into two panels corresponding to the particular polynomial order of approximation and shows the relative errors and the corresponding EOCs. As in the preceding experiments, the obtained errors are small for higher polynomial orders. Furthermore, for piecewise linear (P_1) approximations, we observe that the relative errors indicate a better behavior of EOC, which is expected to be asymptotically $\mathcal{O}(h^2 + \tau^2)$, cf. Remark 4.3. On the other hand, for piecewise quadratic (P_2) approximations, the results for EOC are in a quite good agreement with the derived theoretical estimates of order $\mathcal{O}(h^2 + \tau^2)$, see Theorem 4.1.

σ	M	N	$e^M_{h,2}(P_1)$	EOC	$e^M_{h,2}(P_2)$	EOC
	25	32	$1.0809\text{e}-02$	—	$1.9396\text{e}-03$	—
	50	64	$2.8993\text{e}-03$	1.898	$3.7858\text{e}-04$	2.357
	100	128	$7.3792\text{e}-04$	1.974	$9.4999\text{e}-05$	1.995
0.15	200	256	$1.8625\text{e}-04$	1.986	$2.4025\text{e}-05$	1.983
	400	512	$4.6977\text{e}-05$	1.987	$6.0775\text{e}-06$	1.983
	800	1024	$1.2125\text{e}-05$	1.954	$1.7688\text{e}-06$	1.781
	25	32	$1.1160\text{e}-02$	—	$5.0132\text{e}-03$	—
	50	64	$5.2351\text{e}-03$	1.092	$2.4678\text{e}-03$	1.022
	100	128	$2.3360\text{e}-03$	1.164	$7.3282\text{e}-04$	1.752
0.01	200	256	$4.9604\text{e}-04$	2.236	$1.5149\text{e}-04$	2.275
	400	512	$1.6437\text{e}-04$	1.593	$3.5482\text{e}-05$	2.094
	800	1024	$3.6928\text{e}-05$	2.154	$9.9957\text{e}-06$	1.828

Table 3. Relative errors in L^2-norm and experimental orders of convergence for P_1 and P_2 approximations on the sequences of meshes.

These facts confirm that the DG method combined with the two-stage implicit-explicit scheme is very efficient. In comparison with the approach from [7], where the evaluation of the integral term at the current time step is overcome by Picard iterations, the proposed scheme has the same order of convergence, but needs fewer operations to pass to the next time level. The same conclusions can be stated also for a fixed-point iteration method from [11].

5.4. Greeks. To conclude this section, we show also the robustness of the proposed numerical scheme within a simple sensitivity measurement (commonly called Greeks of an option). The basic sensitivity measures are the first and second derivatives of an option value with respect to the underlying asset, called Delta (i.e., $\partial V/\partial S$) and Gamma (i.e., $\partial^2 V/\partial S^2$), respectively. Delta values are particularly important in hedging portfolios consisting of options while Gamma values play an important role in the corrections for the convexity of an option value.

Considering the quadratic polynomial approximation, the approximate Delta and Gamma values can be directly computed from the derivatives of the basis functions $\{\varphi_j'\}_{j=1}^{\mathrm{DOF}}$ and $\{\varphi_j''\}_{j=1}^{\mathrm{DOF}}$ using the relation (2.5). Figure 1 records these values together with the option prices at the last time level with a particular choice of grid steps. One can easily observe that these plots are of good quality without spurious oscillations, just the non-smooth character in the graph of Gamma values is caused by the piecewise constant basis $\{\varphi_j''\}_{j=1}^{\mathrm{DOF}}$.

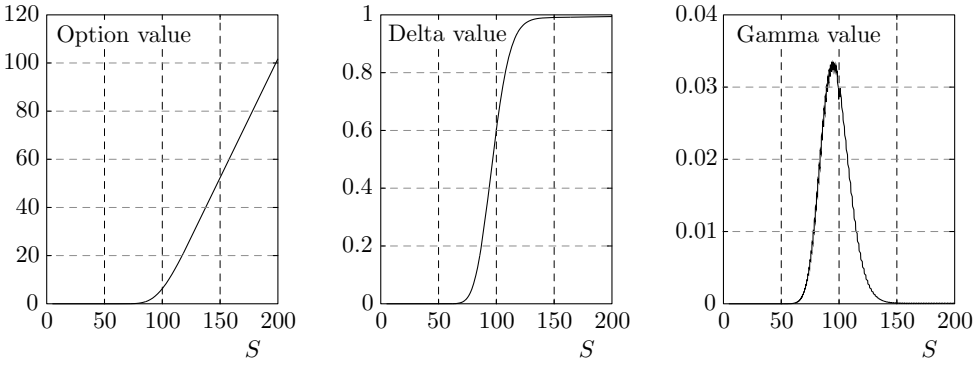

Figure 1. The approximate option values (left), Delta values (middle) and Gamma values (right) evaluated at $\hat{t} = T$ for grid steps $M = 200$ and $N = 256$ ($\sigma = 0.15$).

From this point of view, the depicted values reflect a realistic expectation and reveal the robustness of the presented approach. The detailed error analysis of selected sensitivity measures within the DG method will be the subject of future research.

6. Conclusion

Option pricing methods lead to the analytical solution only under specific circumstances. In other cases, a suitable numerical approximation must be adopted. In this contribution we have developed the DG scheme for the case of the Merton jump-diffusion model considering plain vanilla options. The experimental study provides a quite good convergence and shows that the DG approach is promising even when Lévy models with finite activity of jumps are considered. Obviously, the pricing scheme could be further analyzed within the sensitivity measurement and also extended to options with more complex payoff functions.

References

[1] *Y. Achdou, O. Pironneau*: Computational Methods for Option Pricing. Frontiers in Applied Mathematics 30, Society for Industrial and Applied Mathematics (SIAM), Philadelphia, 2005. zbl MR doi

[2] *A. Almendral, C. W. Oosterlee*: Numerical valuation of options with jumps in the underlying. Appl. Numer. Math. *53* (2005), 1–18. zbl MR doi

[3] *L. Andersen, J. Andreasen*: Jump-diffusion processes: volatility smile fitting and numerical methods for option pricing. Rev. Deriv. Res. *4* (2000), 231–262. zbl doi

[4] *A. Bensoussan, J.-L. Lions*: Impulse Control and Quasi-Variational Inequalities. Gauthier-Villars, Paris, 1984. MR

[5] *F. Black, M. Scholes*: The pricing of options and corporate liabilities. J. Polit. Econ. *81* (1973), 637–654. zbl MR doi

[6] *P. Boyle, M. Broadie, P. Glasserman*: Monte Carlo methods for security pricing. J. Econ. Dyn. Control *21* (1997), 1267–1321. zbl MR doi

[7] *P. Carr, A. Mayo*: On the numerical evaluation of option prices in jump diffusion processes. Eur. J. Finance *13* (2007), 353–372. doi

[8] *R. Cont, P. Tankov*: Financial Modelling with Jump Processes. Chapman & Hall/CRC Financial Mathematics Series, Chapman and Hall/CRC, Boca Raton, 2004. zbl MR doi

[9] *R. Cont, E. Voltchkova*: A finite difference scheme for option pricing in jump diffusion and exponential Lévy models. SIAM J. Numer. Anal. *43* (2005), 1596–1626. zbl MR doi

[10] *J. C. Cox, S. A. Ross, M. Rubinstein*: Option pricing: a simplified approach. J. Financ. Econ. *7* (1979), 229–263. zbl MR doi

[11] *Y. d'Halluin, P. A. Forsyth, K. R. Vetzal*: Robust numerical methods for contingent claims under jump diffusion processes. IMA J. Numer. Anal. *25* (2005), 87–112. zbl MR doi

[12] *V. Dolejší, M. Feistauer*: Discontinuous Galerkin Method. Analysis and Applications to Compressible Flow. Springer Series in Computational Mathematics 48, Springer, Cham, 2015. zbl MR doi

[13] *V. Dolejší, M. Vlasák*: Analysis of a BDF-DGFE scheme for nonlinear convection-diffusion problems. Numer. Math. *110* (2008), 405–447. zbl MR doi

[14] *M. Feistauer, K. Švadlenka*: Discontinuous Galerkin method of lines for solving nonstationary singularly perturbed linear problems. J. Numer. Math. *12* (2004), 97–117. zbl MR doi

[15] *L. Feng, V. Linetsky*: Pricing options in jump-diffusion models: an extrapolation approach. Oper. Res. *56* (2008), 304–325. zbl MR doi

[16] *E. G. Haug*: The Complete Guide to Option Pricing Formulas. McGraw-Hill, New York, 2006.

[17] *F. Hecht*: New development in freefem++. J. Numer. Math. *20* (2012), 251–265. zbl MR doi

[18] *J. Hozman*: Analysis of the discontinuous Galerkin method applied to the European option pricing problem. AIP Conf. Proc. *1570* (2013), 227–234. doi

[19] *J. Hozman, T. Tichý*: On the impact of various formulations of the boundary condition within numerical option valuation by DG method. Filomat *30* (2016), 4253–4263. zbl MR doi

[20] *J. Hozman, T. Tichý*: DG method for numerical pricing of multi-asset Asian options—the case of options with floating strike. Appl. Math., Praha *62* (2017), 171–195. zbl MR doi

[21] *J. Hozman, T. Tichý*: DG method for the numerical pricing of two-asset European-style Asian options with fixed strike. Appl. Math., Praha *62* (2017), 607–632. zbl MR doi

[22] *J. Hozman, T. Tichý*: DG framework for pricing European options under one-factor stochastic volatility models. J. Comput. Appl. Math. *344* (2018), 585–600. zbl MR doi

[23] *A. Itkin*: Pricing Derivatives Under Lévy Models. Modern Finite-Difference and Pseudo-Differential Operators Approach. Pseudo-Differential Operators. Theory and Applications 12, Birkhäuser/Springer, Basel, 2017. zbl MR doi

[24] *S. G. Kou*: A jump-diffusion model for option pricing. Manage. Sci. *48* (2002), 1086–1101. zbl doi

[25] *A. Kufner, O. John, S. Fučík*: Function Spaces. Monographs and Textsbooks on Mechanics of Solids and Fluids. Mechanics: Analysis. Noordhoff International Publishing, Leyden; Academia, Praha, 1977. zbl MR

[26] *Y. Kwon, Y. Lee*: A second-order finite difference method for option pricing under jump-diffusion models. SIAM J. Numer. Anal. *49* (2011), 2598–2617. zbl MR doi

[27] *M. D. Marcozzi*: An adaptive extrapolation discontinuous Galerkin method for the valuation of Asian options. J. Comput. Appl. Math. *235* (2011), 3632–3645. zbl MR doi

[28] *A.-M. Matache, T. von Petersdorff, C. Schwab*: Fast deterministic pricing of options on Lévy driven assets. M2AN, Math. Model. Numer. Anal. *38* (2004), 37–71. zbl MR doi

[29] *R. C. Merton*: Theory of rational option pricing. Bell J. Econ. Manage. Sci. *4* (1973), 141–183. zbl MR

[30] *R. C. Merton*: Option pricing when underlying stock returns are discontinuous. J. Financ. Econ. *3* (1976), 125–144. zbl doi
[31] *D. P. Nicholls, A. Sward*: A discontinuous Galerkin method for pricing American options under the constant elasticity of variance model. Commun. Comput. Phys. *17* (2015), 761–778. zbl MR doi
[32] *W. H. Reed, T. R. Hill*: Triangular Mesh Methods for the Neutron Transport Equation. Technical Report LA-UR-73-479, Los Alamos Scientific Laboratory, New Mexico, 1973; Available at `https://www.osti.gov/servlets/purl/4491151` .
[33] *B. Rivière*: Discontinuous Galerkin Methods for Solving Elliptic and Parabolic Equations. Theory and Implementation. Frontiers in Applied Mathematics 35, Society for Industrial and Applied Mathematics (SIAM), Philadelphia, 2008. zbl MR doi
[34] *H.-G. Roos, M. Stynes, L. Tobiska*: Numerical Methods for Singularly Perturbed Differential Equations. Convection-diffusion and Flow Problems. Springer Series in Computational Mathematics 24, Springer, Berlin, 1996. zbl MR doi
[35] *M. Vlasák*: Time discretizations for evolution problems. Appl. Math., Praha *62* (2017), 135–169. zbl MR doi
[36] *M. Vlasák, V. Dolejší, J. Hájek*: A priori error estimates of an extrapolated space-time discontinuous Galerkin method for nonlinear convection-diffusion problems. Numer. Methods Partial Differ. Equations *27* (2011), 1456–1482. zbl MR doi
[37] *P. Wilmott, J. Dewynne, S. Howison*: Option Pricing: Mathematical Models and Computation. Financial Press, Oxford, 1995. zbl
[38] *K. Zhang, S. Wang*: A computational scheme for options under jump diffusion processes. Int. J. Numer. Anal. Model. *6* (2009), 110–123. zbl MR

Authors' addresses: *Jiří Hozman*, Technical University of Liberec, Faculty of Science, Humanities and Education, Department of Mathematics and Didactics of Mathematics, Studentská 1402/2, 461 17 Liberec, Czech Republic, e-mail: `jiri.hozman@tul.cz`; *Tomáš Tichý*, VŠB-TU Ostrava, Faculty of Economics, Department of Finance, Sokolská třída 33, 702 00 Ostrava, Czech Republic, e-mail: `tomas.tichy@vsb.cz`; *Miloslav Vlasák*, Charles University, Faculty of Mathematics and Physics, Department of Numerical Mathematics, Sokolovská 83, 186 75 Praha 8, Czech Republic, e-mail: `vlasak@karlin.mff.cuni.cz`.